Brazilian Journal of Microbiology (2023) 54:1421–1431
https://doi.org/10.1007/s42770-023-01053-8

BACTERIAL, FUNGAL AND VIRUS MOLECULAR BIOLOGY - RESEARCH PAPER

African ZIKV lineage fails to sustain infectivity in an in vitro mimetic urban cycle

Bárbara Floriano Molina[1] · Nayara Nathiê Marques[1] · Cíntia Bittar[1,2] · Mariana Nogueira Batista[2] · Paula Rahal[1]

Received: 20 September 2022 / Accepted: 27 June 2023 / Published online: 17 July 2023

Abstract

Zika virus (ZIKV) is an arbovirus maintained in nature in two distinct cycles of transmission: urban and sylvatic. Each cycle includes specific vertebrate and invertebrate hosts, and through alternate infections, a conserved consensus sequence is maintained that might vary depending on the cycle. The current study aimed to investigate the ability of ZIKV^{AF} and ZIKV^{BR} to maintain an infectious cycle by alternating passages in cells mimicking the urban (UC) and semi-sylvatic (SC) cycles. The complete genome of the original inoculum and the last passages for each cycle were sequenced by Sanger. Ten passages were performed, as planned, for ZIKV^{BR} UC, ZIKV^{AF} SC, and ZIKV^{BR} SC. ZIKV^{BR} SC showed significant variation in viral titers along the passages, suggesting that the virus is not well adapted to the non-human primate host. ZIKV^{AF} passage in UC was abrogated in the third passage, showing the inability of the African lineage to sustain cycles in human cells, suggesting a low capacity to establish an urban cycle. Several mutations were found in both strains along the passages, but not occurring at equivalent positions. Further studies are needed to elucidate whether any of these specific mutations affect viral fitness.

Keywords Brazilian ZIKV strain · African ZIKV strain · Viral mutations · Host alternation

Introduction

Zika virus (ZIKV) was identified in 1947 in Africa [1, 2], but only became a public global concern after the 2015 outbreak in Brazil, when it was associated with more severe clinical manifestations, such as Guillain-Barré syndrome (GBS) and neurological abnormalities in fetuses and newborns, known as congenital Zika syndrome (CZS) [3–7]. Zika virus belongs to the *Flaviviridae* family that includes other arthropod-borne viruses (arboviruses) like Dengue virus (DENV), West Nile virus (WNV), and Yellow Fever virus (YFV) [8, 9]. The ZIKV genome comprises a 10.8 kb single-stranded positive-sense RNA molecule, which contains a single open reading frame (ORF) flanked by 5' and 3' untranslated regions (UTRs) [10]. The coded single polyprotein is later processed into individual structural and nonstructural proteins: the capsid (C), precursor membrane (prM), and envelope protein (E); NS1, NS2A, NS2B, NS3, NS4A, NS4B, and NS5 [11].

ZIKV infection has been reported and the virus isolated all over the globe, with strains being clustered into two major lineages: African and Asian [12, 13]. The African lineage derives from the monkey Rhesus sample MR-766 (Uganda,

Bárbara Floriano Molina and Nayara Nathiê Marques contributed equally to this work and should be considered joint first authors.

Responsible Editor: Flavio Guimaraes Fonseca

✉ Mariana Nogueira Batista
mnogueirab@rockefeller.edu

Bárbara Floriano Molina
barbaraflorianomolina@gmail.com

Nayara Nathiê Marques
nayara.marques@unesp.br

Cíntia Bittar
cibittar@gmail.com

Paula Rahal
prahal@ibilce.unesp.br

[1] Laboratório de Estudos Genômicos, Departamento de Biologia, Instituto de Biociências Letras E Ciências Exatas (IBILCE), Universidade Estadual Paulista (Unesp), São José Do Rio Preto, Brazil

[2] The Rockefeller University, 1230 York Ave, Manhattan, New York, NY 10065, USA

1947) and comprises many strains isolated from mosquitoes. The Asian lineage is anchored by P6-740 (Malaysia, 1966) and was spread through the Pacific Islands to the Americas, causing the recent human epidemics [11, 14–16]. The main ZIKV route of transmission is by infected *Aedes* sp. mosquito bites, which takes place through two well-established transmission cycles in nature: urban and sylvatic. The urban cycle includes virus circulation mainly in *Aedes aegypti* and humans, while the sylvatic cycle is established between old world monkeys and *Aedes africanus* [17, 18]. To date, there are no records of *Aedes albopictus* taking part in sylvatic cycles, only urban [18].

The alternating passage through distinct hosts balances the consensus sequence of most arboviruses in nature, since transmission and replication in vertebrate and invertebrate hosts are under different selective pressures [19–22]. According to the trade-off hypothesis, allowing sustained replication in a single host results in fitness loss in an alternative host, while alternate infections at sub-optimal fitness levels in each species may allow efficient replication in both [23]. Despite the conserved genome in nature, ZIKV exhibits a high mutational rate in comparison to cellular organisms due to the lack of proofreading activity from the RNA-dependent RNA polymerase (RdRp) and circulates as a quasispecies, with point mutations that may enable successful adaptation to new niches and hosts [22, 24]. Although the two cycles are well established, questions about spillover from the sylvatic cycle to the urban cycle and spillback are still poorly understood. In addition, questions related to the immune restrictions imposed by each host and whether an optimal viral sequence could circulate in different vertebrate hosts remain unanswered. Thus, the aim of the current study was to investigate the ability of ZIKV^{AF} to complete its viral cycle in humans and persist as a continued human-to-human cycle, and the ability of ZIKV^{BR} to complete its viral cycle in non-human primate cells.

Results

Viral adaptation by alternating host

For the Brazilian ZIKV strain, all ten passages of both cycles (ZIKV^{BR} UC and SC) were performed. Most ZIKV^{BR} passages in mammalian cells did not cause cytopathic effects (CPE), considering CPE as the viral ability to lyse cells. In those passages where CPE was identified, it was visible only on the last day of infection. Mosquito cells never showed CPE. Under the semi-sylvatic cycle, ZIKV^{BR} showed high viral titer fluctuation throughout the passages, reaching higher titers in mosquito cells and lower in mammalian cells. However, the strategy seemed to adapt the virus to this host, as shown by the slight increase in viral titers over time in LLC-MK2 cells. For the urban cycle, the virus showed more stability during the passages in the different hosts, with reduced titers only observed in P01, P05, and P10 (Fig. 1).

ZIKV^{AF} completed all ten passages of the semi-sylvatic cycle and viral titers ranged from 10^5 to 10^6 PFU/mL, as seen in Fig. 2. Cytopathic effects were observed on the last day of infection when passaged in LLC-MK2 cells. Unlike the results found in ZIKV^{BR}, ZIKV^{AF} was not able to maintain an urban cycle and only three passages could be performed alternating human and mosquito cells, since no plaques were observed when titrating the supernatant from passage three (Fig. 2, yellow line). To better understand these results, we repeated the experiment from the beginning, and again no plaques were observed when titrating passage three (Fig. 2, green line). Titration of passage three was performed at least three times with no plaque formation. Since no virus was identified by plaque assay, in order to assess whether no virus was produced in passage 3 from the ZIKV^{AF} UC or whether the virus was being produced but was no longer able to cause cell lysis, we performed a titration by indirect immunofluorescence using 4G2 antibody.

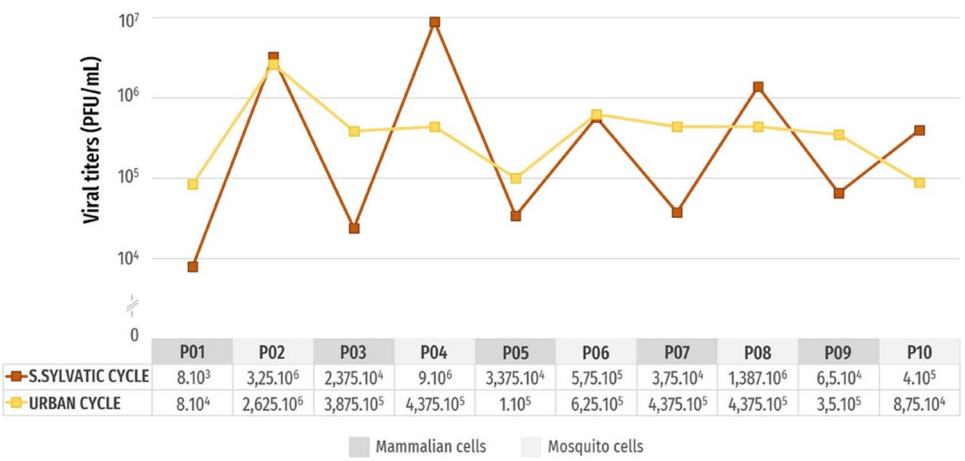

	P01	P02	P03	P04	P05	P06	P07	P08	P09	P10
S.SYLVATIC CYCLE	8.10^3	$3,25.10^6$	$2,375.10^4$	9.10^6	$3,375.10^4$	$5,75.10^5$	$3,75.10^4$	$1,387.10^6$	$6,5.10^4$	4.10^5
URBAN CYCLE	8.10^4	$2,625.10^6$	$3,875.10^5$	$4,375.10^5$	1.10^5	$6,25.10^5$	$4,375.10^5$	$4,375.10^5$	$3,5.10^5$	$8,75.10^4$

Fig. 1 Viral titers of the ZIKV^{BR} alternate passages. Passages of Brazilian ZIKV strain in C6/36, HEK-293, or LLC-MK2. Orange lines represent semi-sylvatic cycle (SC) and yellow lines urban cycle (UC). The letter "P" is the abbreviation for passage and the corresponding number. Odd numbers indicate passages in human (UC) or monkey cells (SC) and even numbers indicate passage in mosquito cells

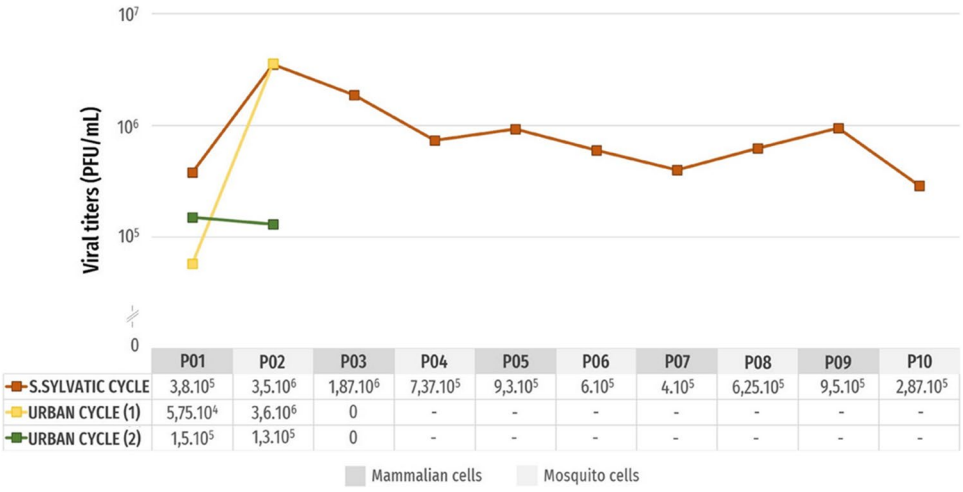

Fig. 2 Viral titers of the ZIKV^{AF} alternate passages. Passages of African ZIKV strain in C6/36, HEK-293, or LLC-MK2. Orange lines represent semi-sylvatic cycle (SC). Yellow and green lines correspond to first and second experiments of the urban cycle (UC) respectively. The letter "P" is the abbreviation for passage and the corresponding number. Odd numbers indicate passages in human (UC) or monkey cells (SC) and even numbers indicate passage in mosquito cells

Only one fluorescent focus was detected in cells infected with undiluted supernatant, corresponding to a titer of 0.6 PFU/mL (Fig. 3).

Mutations in ZIKVBR from UC and SC

The ZIKV^{BR} initial inoculum genome sequence obtained was 10.679nt in length, with the 5'UTR 48nt and the 3'UTR 365nt long (GenBank OK569755). The annotation of each genomic region was determined based on the sequence NC_035889.1. The consensus viral sequences obtained from each cycle after ten passages (ZIKV^{BR} SC P10 and UC P10 – GenBank OK569756 and OK569757 respectively) were analyzed and both resulted in 10.677nt in length, with a 5'UTR of 48nt and a 3'UTR of 363nt. When compared to the initial inoculum sequence, it was possible to observe the emergence of mutations at the nucleotide and amino acid levels distributed throughout the genome (Fig. 4A). All mutations identified appeared as ambiguities in the electropherogram, probably due to the quasispecies nature of the RNA virus, with genomes presenting different nucleotides at specific sites composing the viral population.

At the end of the ZIKV^{BR} SC passages, ten nucleotide mutations were identified, six of which may result in amino acid change (Fig. 4B). For example, G1062A/G – the 1062 nucleotide of the initial inoculum was guanine (G) and in the SC-adapted virus adenine (A) was observed as well as guanine; so, in those sequences that carry an adenine as the 1062 nucleotide there is amino acid mutation from Glycine to Serine, but for those that still carry guanine no change has occurred and the amino acid is still Glycine. Thus, the codons that may result in amino acid change from the SC adaptation were as follows: G**319**S/G at the E protein (Glycine → Serine/Glycine); L**1041**L/F at NS1 (Leucine → Leucine/Phenylalanine); V/A**1263**A/V at NS2A (Valine/Alanine → Alanine/Valine); I**1275**L/I at NS2A (Isoleucine → Leucine/Isoleucine); S**1443**S/R at NS2B (Serine → Serine/Arginine); K**2089**K/Q at NS3 (Lysine → Lysine/Glutamine). The other four nucleotides that exhibited ambiguities but did not result in amino acid mutations were as follows: T**467**T/C (Alanine at the 120 residue of the coding region—located at the Capsid protein); C**4127**C/T (Asparagine at 1340 residue—NS2A);

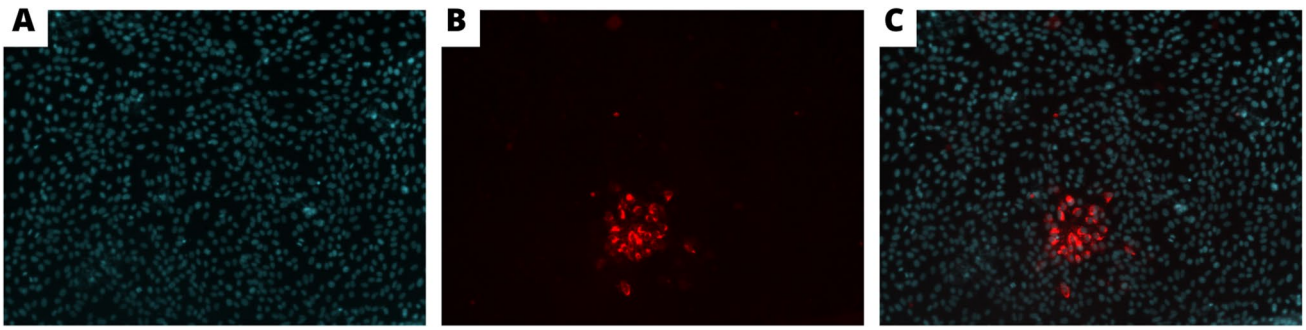

Fig. 3 ZIKV^{AF} quantification by immunofluorescence assay. Performed with virus from the third passage of the urban cycle using ZIKV^{AF}. **A** Blue: DAPI, staining nuclei. **B** Red: 4G2, staining ZIKV. **C** Merge of the **A** and **B** images

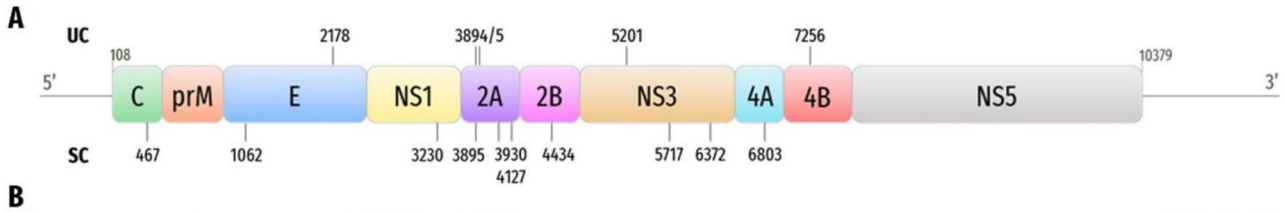

B

Position	n	aa	n	aa	n	aa	n	aa	n	aa	n	aa	n	aa
	467	120	632	175	997	297	1062	319	1162	352	2178	691	3230	1041
ZIKV^{BR} Initial inoculum	T	Ala	**C/T**	Cys	**G/A**	Ser/Asn	G	Gly	**A/G**	Glu/Gly	C	His	A	Leu
ZIKV^{BR} UC	T	Ala	C	Cys	G	Ser	G	Gly	A	Glu	**T/C**	Tyr/His	A	Leu
ZIKV^{BR} SC	**T/C**	Ala	C	Cys	G	Ser	**A/G**	Ser/Gly	A	Glu	C	His	**A/T**	Leu/Phe

Position	n	aa	n	aa	n	aa	n	aa	n	aa	n	aa	n	aa
	3894	1263	3895	1263	3930	1275	4127	1340	4434	1443	4724	1539	5201	1698
ZIKV^{BR} Initial inoculum	G	Val	**T/C**	Val/Ala	A	Ile	C	Asn	A	Ser	**A/G**	Gly	T	Pro
ZIKV^{BR} UC	**A/G**	Thr/Ala	**C/T**	Thr/Met	A	Ile	C	Asn	A	Ser	A	Gly	**T/C**	Pro
ZIKV^{BR} SC	G	Ala	**C/T**	Ala/Val	**C/A**	Leu/Ile	**C/T**	Asn	**A/C**	Ser/Arg	A	Gly	T	Pro

Position	n	aa	n	aa	n	aa	n	aa	n	aa	n	aa
	5717	1870	6372	2089	6803	2232	7256	2383	7357	2417	7360	2418
ZIKV^{BR} Initial inoculum	C	Asn	A	Lys	C	Phe	T	Ile	**T/G**	Val/Gly	**T/G**	Val/Gly
ZIKV^{BR} UC	C	Asn	A	Lys	C	Phe	**T/G**	Ile/Met	T	Val	T	Val
ZIKV^{BR} SC	**T/C**	Asn	**A/C**	Lys/Gln	**C/T**	Phe	T	Ile	T	Val	T	Val

Fig. 4 Mutations emerged after UC and SC alternate passages in ZIKV^{BR} genome. **A** Graphic representation of the ZIKV^{BR} genome indicating the observed nucleotide mutations for UC (top) and SC (bottom). **B** Nucleotide and amino acid mutations in the genome of ZIKV^{BR} UC and SC: n, nucleotide position; aa, amino acid position. Bold nucleotides with slashes (/) between represent both nucleotides identified in each position. Positions in relation to GenBank NC_035889.1 sequence. The colored regions indicate the genomic region where the mutation is located

C**5717**T/C (Asparagine at 1870—NS3); and C**6803**C/T (Phenylalanine at 2232—NS4A).

ZIKV^{BR} UC final virus presented five sites of the genome with two possible nucleotides, one of them was a synonym substitution T**5201**T/C (Proline at the 1698 residue of the coding region, located at NS3). The other four resulted in amino acid mutations at three codons: H**691**Y/H at the E protein (Histidine → Tyrosine/Histidine); V/A**1263**T/M/A/V at NS2A (Valine/Alanine → Threonine/Methionine/Alanine/Valine); I**2383**I/M at NS4B (Isoleucine → Isoleucine/Methionine). The nucleotides 3894 and 3895 belong to the same codon and mutations were found in both, enabling the observation of four possible amino acids residing at position 1263: Threonine, Methionine, Valine, and Alanine (Fig. 4B).

The initial inoculum also showed variations along the genome, with ambiguities in seven nucleotides (Fig. 4B). These variations did not appear at the corresponding locations in the adapted ZIKV^{BR} genomes, suggesting that the adaptation strategy purified the viral population towards a more homogeneous population in those specific nucleotides. The nucleotide 3895 was the only one that had ambiguities in the initial and also in the adapted sequences, resulting in two possible amino acids at the 1263 initial residue (Valine and Alanine).

Mutations in ZIKVAF from UC and SC

Sequencing of the initial inoculum of ZIKV^{AF} resulted in a complete genome sequence of 10.656nt, comprising a 5′UTR of 52nt and a 3′UTR 351nt in length (GenBank OK569758). Genomic regions were determined based on sequence NC012532 as shown in Fig. 5A.

The consensus sequence obtained from the tenth passage of the semi-sylvatic cycle has 10.668nt, with 24nt in the 5′UTR and 363nt in the 3′UTR (GenBank OK569759). In the urban cycle, the complete genome of final passage two was sequenced, resulting in a consensus sequence of 10.625 n, with a 5′UTR of 20 bp and a 3′UTR of 354 bp (GenBank OK569760). It was not possible to sequence the virus from passage three.

In Fig. 5B, there is a description of the mutations found in each cycle. For the semi-sylvatic cycle, changes were observed at six nucleotides. Of these, a non-synonymous substitution was observed at residue L**1263**F at NS2A (Leucine → Phenylalanine). Another four mutations occurred in nucleotide sites that presented ambiguities in the electropherogram, three of which did not generate an amino acid change: C**5599**C/T and A**5608**A/C (both in NS3), G**8128**G/A and A**8129**G (both in NS5 protein), the

A

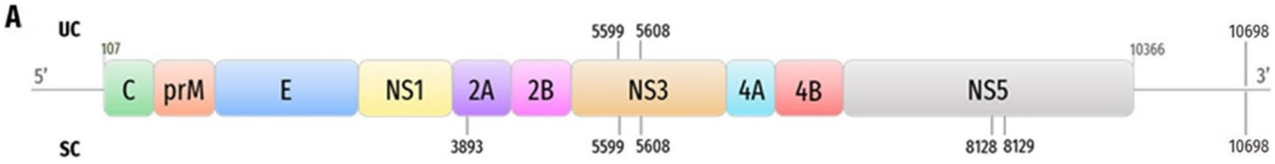

B

Position	n	aa	n	aa	n	aa	n	aa	n	aa	n	aa
	3893	1263	5599	1865	5608	1869	8128	2709	8129	2710	10698	-
$ZIKV^{AF}$ Initial inoculum	C	Leu	C	Iso	A	Thr	G	Glu	A	Thr	-	-
$ZIKV^{AF}$ UC	C	Leu	**C/T**	Iso	**A/C**	Thr	G	Glu	A	Thr	**C**	-
$ZIKV^{AF}$ SC	**T**	Phe	**C/T**	Iso	**A/C**	Thr	**G/A**	Glu	**A/G**	Thr/Ala	**C**	-

Fig. 5 Mutations emerged after UC and SC alternate passages in $ZIKV^{AF}$ genome. **A** Graphic representation of the $ZIKV^{AF}$ genome indicating the observed nucleotide mutations for UC (top) and SC (bottom). **B** Nucleotide and amino acid mutations in the genome of $ZIKV^{AF}$ UC and SC: n, nucleotide position; aa, amino acid position. Bold nucleotides with slashes (/) between represent both nucleotides identified in each position. Positions in relation to GenBank NC_012532.1 sequence. The colored regions indicate the genomic region where the mutation is located

latter being a non-synonymous substitution resulting in the exchange of a Threonine Alanine/Threonine at the 2710 amino acid residue of the coding region. Finally, in the 3′UTR region, at position **10698**, a cytosine was inserted.

At the end of the UC passages, three mutations were observed and none of them resulted in amino acid exchanges. Two of these mutations were observed in a position of ambiguities at the electropherogram, C**5599**C/T and A**5608**A/C (both in NS3). An insertion of cytosine at position **10698** was also observed in this cycle.

Discussion

Endemic strains of arboviruses arose in humans from evolutionarily distinct enzootic cycles, such as ZIKV, DENV, CHIKV, and YFV, where the virus circulates among arboreal *Aedes* sp. vectors and non-human primate hosts. They evolved into peri-urban cycles in zones of emergence and were finally able to establish urban cycles, usually between *Aedes* sp. mosquitoes and humans [17, 25, 26]. Phylogenetic analysis revealed that the endemic ZIKV strain circulating in Brazil is related to Asian strains that spread across the Pacific and were responsible for the first and most recent outbreaks of the disease in humans [13, 14, 27, 28].

$ZIKV^{BR}$ alternate passages mimicking the urban cycle showed low variation in viral titers, which evidences the stability of the $ZIKV^{BR}$ urban transmission between human and *Aedes* mosquitoes. These results reinforce the evidence that the contemporary Asian strains of the virus established a successful urban cycle and rapidly spread all over the world, which is corroborated by NS1 codon usage adaptation to human housekeeping genes in the Asian pandemic lineage [29]. The ten passages simulating the sylvatic cycle show that the strain is also able to infect non-human primate kidney cells. The fluctuation in titers along the passages of the SC contrasts with the demonstrated stability of the UC, with the highest titers of the SC being observed in mosquito cells. The infection in monkey cells resulted in lower viral titer in comparison to mosquito cells, suggesting that the virus is not yet well adapted to the mammalian non-human host and that the immune restrictions imposed by mosquito cells might require less adaptation than those imposed by mammalian cells.

$ZIKV^{BR}$ SC results draw attention to the possibility of the emergence of a $ZIKV^{BR}$ enzootic cycle—since the "spill-back" phenomenon is an ecological process that has previously occurred in other arboviruses, such as YFV when it arrived in the Americas [17, 30]. Althouse and colleagues [17] developed a mathematical model based on many biological parameters to assess the ZIKV potential to establish a sylvatic cycle in the Americas and showed that the persistence depends on vector and host population sizes, host birthrates, and viral force of infection. The strains that caused the recent ZIKV outbreak have already been detected in non-human primates in Brazil [31–33]. Terzian and colleagues inoculated *C. penicillata* with ZIKV American strains, proving sustained viremia. The authors also detected the virus in *A. aegypti* that inhabits the same area as monkeys which tested positive for the ZIKV American strain. Another study, with two neotropical primate species that live close to humans in South America, demonstrated that both are susceptible to ZIKV infection. The authors reported viremia without signs of disease and seroconversion in 28 days [34]. Thus, it is urgent to understand the potential for the establishment and persistence of a ZIKV enzootic cycle in the Americas which might impact public health policies to control the virus circulation. For future

studies that aim to investigate spillback in vitro, we suggest using cell lines of New World primates to mimic the sylvatic cycle, instead of LLC-MK2, which is originally from Old World monkeys.

Regarding the ZIKV^{AF} semi-sylvatic cycle, we observed stability of the virus titer throughout the ten passages, which supports the natural history of the virus that was discovered in Africa circulating between monkeys and mosquitoes and has documented enzootic transmission [2]. In parallel, the ZIKV^{AF} urban cycle was interrupted at the third passage since it was not possible to identify viruses by plaque assay and only one focus (0.6 FFU titer) was identified by immunofluorescence assay, indicating a possible loss of viral infectivity.

It is interesting, however, that along the ZIKV^{AF} UC coding region, only synonymous mutations were observed and one insertion at the 3'UTR was found in the virus recovered from the second passage. The 3'UTR from flaviviruses is described to have importance in coordinating replication and virus assembly and mutations in this region are shown to impair virus fitness [35], while mutations in YFV 3'UTR are related to attenuation [36]. However, this seems not to be the case here since the exact same insertion was found in the semi-sylvatic cycle which did not display any signs of attenuation. One possibility is that this is an adaptive mutation related to the mosquito cells (C6/36), which were used in both cycles. Probably, due to limitations of the Sanger sequencing technique, which identifies mutations that are present in most populations and not all populations in the sample, it may not have been possible to identify any mutations that could explain the loss of infectivity. Another possibility is that insertion into the 3'UTR in the ZIKV^{AF} UC may have interfered with viral replication; however, no functional investigations were conducted in this study to address this question.

A study with African ZIKV strains showed special codon usage adaptation for the green African monkey when compared to Asian strains, which might reflect the efficient sylvatic transmission of the African strains, as well as a possible peri-urban cycle with asymptomatic transmission [37]. It may also be related to the inability of ZIKV^{AF} to complete the urban cycle adaptation experiments in the present study.

It is not yet clear if the African strains are associated with CZS [38] and some in vivo and in vitro studies demonstrated that African ZIKV has increased fitness and virulence in mosquitoes and vertebrates when compared to Asian strains [39–43]. There are intrinsic differences between the virulence and pathogenicity of African and Asian lineages, as reviewed by Simonin and colleagues [44]. The Asian strain phenotype provides persistent infections, producing less viruses and a lower infection rate, inducing less cell death at early stages and, consequently, being able to reach the fetus' nervous system; while African strains trigger acute infections that end up being noticed more quickly and stopped by the defenses of the organism. These African lineage characteristics may be linked to the lack of human infection cases and associated with more severe syndromes [44]. Thus, our results showing that ZIKV^{AF} failed in passaging between human and mosquito cells, coupled with the reduced number of reports of this lineage infecting humans, suggest that the African lineage might be unable to establish an efficient urban cycle with humans as vertebrate hosts.

Both strains, ZIKV^{BR} and ZIKV^{AF}, had mutations at the nucleotide and amino acid levels, but did not share the same mutation position. The greater number of variations found in the ZIKV^{BR} genomes when compared to the ZIKV^{AF} might be related to the ability of contemporary Asian strains to adapt more easily to only one or a few passages [22]. Furthermore, Haddow et al. (2012) show that the variation found in the ZIKV MR766 strain from Uganda (HQ234498), considered a classic strain and widely used in in vitro research studies that aim to model Zika infections, is between 0.4 and 0.6% when compared to two other variants of MR766 (AY632535 and DQ859059) also isolated from rhesus monkeys in Uganda, proving to be a highly conserved genome [45].

Among the amino acid residues that showed mutations in both ZIKV^{BR} cycles, two are located in the E protein, which is one of the main components for virus-cell recognition: the 319 residue (SC) belongs to Domain I, which is involved in organizing the envelope structure; while 691 (UC) is located in Domain III, which is associated with binding to receptors [16]. The ZIKV^{BR} UC 691 amino acid mutation (H691Y) was observed in a Colombian strain isolated from the serum of a pregnant woman diagnosed with Zika in 2016 by intraperitoneal inoculation into mice [46].

In addition, Shrivastava and collaborators [47] investigated microevolution, seeking variations capable of contributing to viral adaptation to the host. Among the eleven residues found, two of them were 691 and 1263. At position 691 of the amino acid sequence, the authors found the same amino acids as in our study: a Histidine residue or a Tyrosine. These amino acids were also found in two different Asian strains of *Aedes* from Malaysia in 1966. The amino acid 1263 located at NS2A, however, showed two possible variations in several strains: Alanine (A) was observed in two *A. aegypti* samples (from Malaysia 1966 and from Mexico 2016) and Valine (V) in three human-isolated strains (Thailand 2013 and Panama 2015/2016) [47]. The same was found by Strottmann et al. [48] in a study with three Brazilian strains, two of them had Alanine residue and one had Valine at position 1263. In silico analysis showed Valine in five other Asian-derived strains and identified that this mutation also maps to a transmembrane domain [48].

The 1263 residue was the one that varied the most between ZIKV^{BR} strains in the present study. It varies from the

$ZIKV^{BR}$ initial inoculum, having Valine (V) and Alanine (A) within the population. In the $ZIKV^{BR}$ from the SC, the same A and V were present within the SC population. In the UC, there were variations in two nucleotides from the same codon (1st and 2nd positions), resulting in four possible amino acids in the UC P10 population: Threonine (T), Methionine (M), Alanine (A), and Valine (V). The A1263V substitution was found in a Brazilian isolate from Bahia in 2015; the predicted secondary structure containing this amino acid variation was analyzed resulting in inversions between α-helices and coils [49]. Ávila-Perez and colleagues [50] demonstrated that the unique A1263V substitution in the whole genome is responsible for increased virulence in mice (virulence factor considered: the relative capacity of a microorganism to overcome the host's defenses), decreasing host innate immune responses and viral-induced apoptosis in vitro. The nucleotide mutation responsible for threonine at 1263 (G3894A) was found only in a Panama strain isolated in 2015 [51]. These results together indicate that $ZIKV^{BR}$ passage in non-human primates could pressure the virus sequence towards alternative amino acids, with unknown effects.

In $ZIKV^{AF}$ SC adaptation, the only mutation found in NS2A protein was L1263F, which has not previously been found in other studies (note that the 1263 amino acid residue in the ZIKV African genome is not homologous to the 1263 residue in the Asian genome). In the $ZIKV^{BR}$ sequencing analysis, NS2A was the genomic region with the most sites of mutation (4/10); in the work by Strottmann et al. [48], a greater number of mutations was also observed in this protein (4/8), even though they are not the same mutations. Interestingly in $ZIKV^{AF}$ sequences, only one mutation was observed in this protein and it was the only fixed mutation found along the passages. The greater number of variations in NS2A when compared to the rest of the genome might indicate less functional restriction in this genomic region.

$ZIKV^{BR}$ sequences showed no variation along the NS5 genomic region, suggesting the strain is well established for both cycles and agreeing with the nature of the polymerase—the largest (~ 100 kDa) and most conserved protein of the ZIKV genome, with 94% similarity between African and Asian strains [52]. In contrast, $ZIKV^{AF}$ SC showed mutations in two NS5 residues (one synonymous and one non-synonymous T2710T/A), which are adjacent amino acids located between two active sites of the catalytic tetrad from MTase domain—responsible for the 5′ capping and for stabilization of the viral genome [53, 54]. The $ZIKV^{AF}$ NS3 protein was the region that presented the most nucleotide mutations, all synonymous; the same region in the $ZIKV^{BR}$ sequences also showed many variation sites, only one causing amino acid change, K2089K/Q. If any of these non-synonymous mutations are fixed in the viral population, it might impose positive or negative changes in the viral fitness (if not neutral), still to be determined.

With respect to the synonymous variations found in both cycles of $ZIKV^{BR}$/^{AF} strains used in the present study, it should be noted that changes in nucleotide composition are an essential evolutionary mechanism and a sign of viral adaptation to the host [55]. Changes in codon usage after shifting hosts might be required to "fine-tune" the virus-new host interactions [55, 56]. Comparative analysis of the relative synonymous codon usage (RSCU) between ZIKV and hosts indicates that the virus tends to develop a codon usage pattern similar to that of its hosts [57]. According to Wang and collaborators [57], the codon usage bias of the two major ZIKV lineages is relatively low and it is suggested that translational selection and mutation pressure play important roles in shaping the ZIKV codon usage pattern.

Conclusion

Despite performing the same adaptation experiments with the same cellular lineages, the distinct ZIKV strains behaved differently in each cycle. The completion of the ten alternate passages of the semi-sylvatic cycle with the $ZIKV^{BR}$ strain draws attention to its potential to establish an enzootic cycle, while the interruption of the $ZIKV^{AF}$ urban cycle at the third passage might be a sign of inability to adapt to a human host and maintain the urban transmission. Both strains, $ZIKV^{BR}$ and $ZIKV^{AF}$, had mutations at nucleotide and amino acid level, never at the same position. The greater number of variations found in the $ZIKV^{BR}$ genomes when compared to the $ZIKV^{AF}$ might be related to the ability of contemporary Asian strains to adapt more easily to few passages, which reinforces the genetic and phenotypic characteristics intrinsic to each lineage. Further studies are needed to elucidate the viral evolution mechanisms, whether the identified mutations are host adaptations, and their impacts on viral fitness.

Experimental procedures

Cell culture and virus

Aedes albopictus cells (C6/36; ATCC CRL-1660) were cultured in Leibowitz medium (L-15) (Vitrocell) supplemented with 10% fetal bovine serum (FBS) (Cultilab), 100 U/mL of Penicillin, and 100 µg/mL of Streptomycin (P/S) (Thermo Fisher), and incubated at 28 °C in polystyrene culture flasks. The human embryonic kidney (HEK-293; ATCC CRL-1573), *Cercopithecus aethiops* kidney (Vero E6; ATCC CRL-1586), and *Macaca mulata* kidney (LLC-MK2; ATCC CCL-7) cell lineages were grown in high-glucose Dulbecco's Modified Eagle Medium (DMEM) (Cultilab), supplemented with 100 U/mL of Penicillin and 100 µg/mL of Streptomycin (P/S) and 10% FBS. Incubation was carried out in a humid incubator enriched with 5% CO_2 at 37 °C.

Two ZIKV strains were used in this study: an African strain MR766 ($ZIKV^{AF}$) (GenBank NC012532) and BeH815744 ($ZIKV^{BR}$), and a Brazilian strain isolated in Paraiba during the 2015 epidemic, kindly provided by Prof. Dr. Pedro Vasconcelos, Evandro Chagas Institute, Brazil (GenBank KU365780.1).

Virus stocks

In order to produce viral stocks, C6/36 were seeded 24 h before infection and 400 µL of concentrated virus ($ZIKV^{BR}$ and $ZIKV^{AF}$) were inoculated for 1 h, being homogenized every 15 min. Following, L-15 medium supplemented with 1% FBS, 100 U/mL of Penicillin, and 100 µg/mL of Streptomycin (P/S) were added. After 96 h, cells were frozen at − 80 °C for at least 24 h. Next, the flasks were thawed at room temperature, the contents were centrifuged at 4 °C for 5 min at 1361 × g, and the supernatants were filtered through a 0.45 µM syringe filter, aliquoted, and stored at − 80 °C. Virus stocks were subsequently titered as described below. All experiments using replicating viruses were performed in a BSL2 + facility.

Viral adaptation by alternating host

Alternate passages of infection were carried out between human embryonic kidney (HEK-293) and mosquito (C6/36) cell lines, simulating the urban cycle (UC), and passages between monkey (LLC-MK2) and mosquito (C6/36) cell lines, simulating the semi-sylvatic cycle. We used a "semi" sylvatic cycle (SC) because *A. albopictus* is a confirmed vector only in the ZIKV urban cycle and therefore represents a possible zone of emergence component. Cells were seeded under optimal conditions considering each lineage growth rate in order to have healthy and 100% confluent cells at the end of the fourth day of infection. In this way, the seedings were performed so that the flasks reached 30%, 60%, and 80% confluency, respectively, for HEK-293, LLC-MK2, and C6/36 on the first day of infection.

Both cycles were carried out in parallel with the $ZIKV^{AF}$ and $ZIKV^{BR}$ strains separately and the process of viral adaptation by alternating hosts was designed for 10 passages in each cycle (Fig. 6). For each passage, the supernatant was collected, centrifuged for 5 min at 1361 × g at 4 °C, filtered through a 0.45 µM syringe filter, aliquoted, and stored at − 80 °C. For nomenclature purposes, urban cycle passages were named with the following keycode: UC P01, i.e., Urban Cycle Passage 01; the same was used for the semi-sylvatic cycle: SC P01, i.e., Semi-Sylvatic Cycle Passage 01, and so on. All passages were performed using 1×10^3 PFU/mL in both cell hosts. The $ZIKV^{AF}$ UC was performed in independent events in order to verify the result obtained.

Viral titration by plaque assay

All titration steps were performed by plaque assay. VERO E6 cells (2×10^5 cells/well) were seeded 24 h prior to the

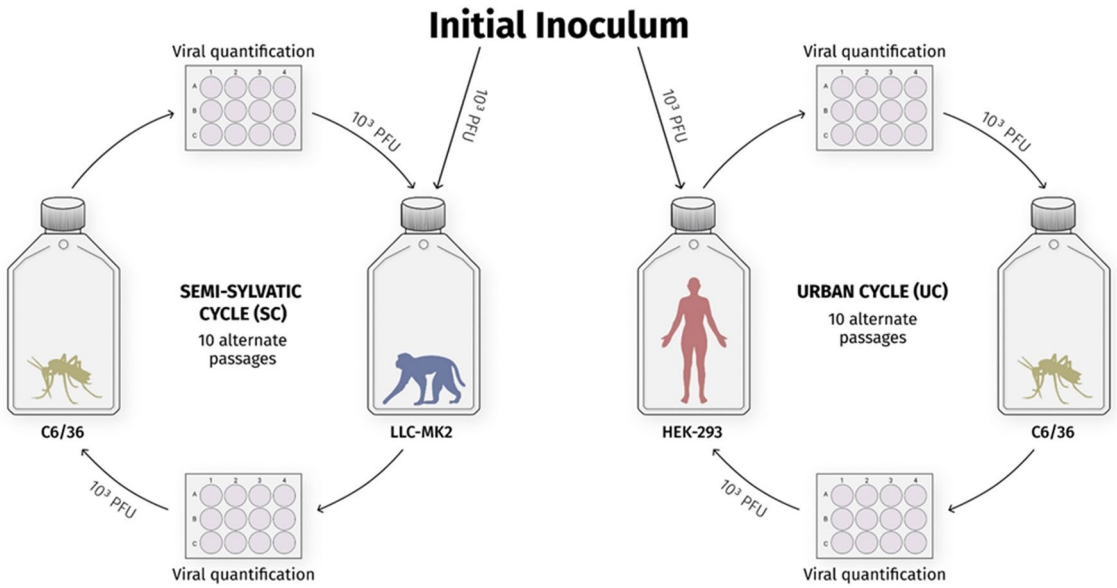

Fig. 6 Experimental design of the in vitro adaptation studies of ZIKV that simulate its transmission cycles. The first infection of each cycle was made from the respective initial inoculum ($ZIKV^{AF}$ or $ZIKV^{BR}$). Both cycles were designed to have ten alternate passages, five performed in cell lines that simulated the invertebrate host and five in the respective vertebrate host cell. Each passage corresponds to the transfer of 10^3 viral particles from the supernatant of the previous passage which was titered by plaque assay

assay in 12-well plates. Afterward, the confluent monolayers were inoculated with 400 µL of serial dilutions (dilution factor 10) of the virus and incubated at 37 °C, homogenizing every 15 min. Each dilution was plated in duplicate. After 1 h, the inoculum was removed and semi-solid CMC medium (1.5% carboxymethyl cellulose/high-glucose DMEM) was added, supplemented with 1% FBS, 100 U/mL of Penicillin, and 100 µg/mL of Streptomycin (P/S). After 96 h of incubation at 37 °C and 5% CO_2, the samples were fixed with 10% formaldehyde for 20 min and stained with 1% crystal violet in a 20% ethanol solution. The viral titer was expressed as plaque-forming units (PFUs) per milliliter. For passages in which the viral titer was significantly different from the expected value, these titrations were repeated at least twice to confirm the result.

Viral titration by indirect immunofluorescence assay

VERO E6 cells (2×10^4 per well) were seeded in 96-well transparent plates 24 h before the assay. The confluent monolayers were inoculated with 50 µL of viral serial dilutions (dilution factor 10) and incubated at 37 °C. After 1 h of adsorption, the inoculum was removed and 190 µL of a semi-solid 1.5% CMC medium was added to each well and incubated for 48 h. At the end of the incubation period, the cells were fixed with 4% paraformaldehyde (PFA) and permeabilized with 0.2% Triton-X/PBS (Sigma-Aldrich) prior to blocking using 3% bovine serum albumin in PBS (BSA – Sigma-Aldrich) for 30 min at RT. Cells were stained using anti-4G2 (MAB10216—Merck) antibody (1:250 in 0.1% BSA/PBS) for 2 h and secondary antibody anti-mouse Alexa Fluor 594—(A12381—Thermo Fisher Scientific) (1:500 in 0.1% BSA/PBS) for 1 h, incubated at room temperature. Nuclei were stained using DAPI (10 mg/mL stock, in 1:7000 in PBS) for 5 min. The fluorescent focus-forming units were analyzed using a fluorescence microscope (Zeiss Axio Vert. A1) and counted in duplicates. The viral titer was expressed in focus-forming units (FFU).

Complete genome amplification

To amplify the complete genome of both ZIKV strains, an amplification strategy was outlined based on overlapping fragments. The most conserved genome regions were mapped and pairs of specific primers capable of covering the entire genome were designed by our group, built on alignments of several viral sequences available on GenBank using BioEdit v7.0.5 software [58] (see Table S1 for NESTED-PCR primers). The annealing temperature of each primer was calculated using the NEB Calculator v1.13.0 [59].

The complete genome of the virus stocks and the virus from the last passage of each cycle were amplified as follows. The extraction of viral RNA was carried out by the TRIzol® Reagent method (Invitrogen) according to the manufacturer's instruction. The synthesis of complementary DNA was performed using the High-Capacity cDNA Reverse Transcription kit (Applied Biosystems) with four specific reverse primers—ZIKV P3R, ZIKV P6R, ZIKV P9R, and ZIKV P12R (see Table S1). For the amplification of the complete ZIKV genome, it was divided into 15 fragments, and NESTED-PCR reactions were designed so that they overlapped, as described in Table S1. The reactions were carried out using Platinum Taq polymerase (Invitrogen) with the addition of DMSO, at a final concentration of 4% and specific primers for each fragment (Table S1). All primers were used at the final concentration of 0.2 pmol/µL. The amplified products were identified by electrophoresis on 1% agarose gel stained with Ethidium bromide (Merck), and analyzed under ultraviolet light (ChemiDoc™ MP Imaging System – BioRad).

Sanger sequencing

PCR products were purified using the Zymo™Gel DNA Clean & Concentrator purification kit (Zymo) according to the manufacturer's recommendations. The sequencing technique used in this study was according to the methodology of Sanger and collaborators [60]. The sequencing was performed on the ABI 3130 XL Genetic Analyzer (Life Technologies). After purification, the sequencing reaction was performed with BigDye Terminator v3.1 (Life Technologies) using the NESTED-PCR primers for each fragment (Table S1). The sequencing reactions for each primer were performed twice in order to optimize coverage.

Genome sequencing analysis

Complete genome sequences were assembled using SeqMan Pro® version 7.1.0 (DNASTAR) with ZIKV refseq NC_012532.1 (GenBank) as a reference sequence. Visual quality analysis was performed throughout the genome and coverage of at least three sequences for each site was considered for the analysis. Finally, the resulting nucleotide and amino acid sequences from stock and each cycle (SC and UC $ZIKV^{AF}$/$ZIKV^{BR}$) were aligned using Clustal W nested in the BioEdit v.7.0.5 [58] package and compared to identify mutations.

Supplementary Information The online version contains supplementary material available at https://doi.org/10.1007/s42770-023-01053-8.

Acknowledgements We thank all the participants who contributed to this study.

Author contribution M. N. B. conceived the study. All authors designed the study. B. F. M., N. N. M., and C. B. performed the experiments and were involved in the acquisition and analysis of the data; all authors were involved in the interpretation of the data. B. F. M. and N. N. M. wrote the manuscript with input from all authors.

Funding This work is supported by the Coordenação de Aperfeiçoamento de Pessoal de Nível Superior—Brazil (CAPES) Finance Code 001.

Data availability The data that support the findings of this study are openly available in GenBank, reference numbers OK569755, OK569756, OK569757, OK569758, OK569759, and OK569760, and in the supplementary material of this article.

Declarations

Ethics approval The study described is exempt from ethics approval.

Conflict of interest The authors declare no competing interests.

References

1. Dick GWA (1953) Epidemiological notes on some viruses isolated in Uganda (Yellow fever, Rift Valley fever, Bwamba fever, West Nile, Mengo, Semliki forest, Bunyamwera, Ntaya, Uganda S and Zika viruses). Trans R Soc Trop Med Hyg 47(1):13–48. https://doi.org/10.1016/0035-9203(53)90021-2
2. Dick GWA, Kitchen SF, Haddow AJ (1952) Zika virus (I). Isolations and serological specificity. Trans Royal Soc Trop Med Hyg 46(5):509–520. https://doi.org/10.1016/0035-9203(52)90042-4
3. França GVAd et al (2018) Síndrome congênita associada à infecção pelo vírus Zika em nascidos vivos no Brasil: descrição da distribuição dos casos notificados e confirmados em 2015–2016. Epidemiologia e Serviços de Saúde 27(2):e2017473. https://doi.org/10.5123/S1679-49742018000200014
4. Cauchemez S et al (2016) Association between Zika virus and microcephaly in French Polynesia, 2013–15: a retrospective study. Lancet 387(10033):2125–2132. https://doi.org/10.1016/S0140-6736(16)00651-6
5. Magalhães-Barbosa MC et al (2016) Trends of the microcephaly and Zika virus outbreak in Brazil, January-July 2016. Travel Med Infect Dis 14(5):458–463. https://doi.org/10.1016/J.TMAID.2016.09.006
6. de Oliveira WK et al (2017) Infection-related microcephaly after the 2015 and 2016 Zika virus outbreaks in Brazil: a surveillance-based analysis. Lancet 390(10097):861–870. https://doi.org/10.1016/J.TMAID.2016.09.006
7. Calvet G et al (2016) Detection and sequencing of Zika virus from amniotic fluid of fetuses with microcephaly in Brazil: a case study. Lancet Infect Dis 16(6):653–660. https://doi.org/10.1016/S1473-3099(16)00095-5
8. Fleming AM et al (2016) Zika virus genomic RNA possesses conserved G-quadruplexes characteristic of the Flaviviridae family. ACS Infect Dis 2(10):674–681. https://doi.org/10.1021/ACSINFECDIS.6B00109/SUPPL_FILE/ID6B00109_SI_001.PDF
9. Weaver SC et al (2016) Zika virus: History, emergence, biology, and prospects for control. Antiviral Res 130:69–80. https://doi.org/10.1016/J.ANTIVIRAL.2016.03.010
10. Kuno G, Chang GJ (2007) Full-length sequencing and genomic characterization of Bagaza, Kedougou, and Zika viruses. Arch Virol 152(4):687–696. https://doi.org/10.1007/S00705-006-0903-Z
11. Wang A et al (2017) Zika virus genome biology and molecular pathogenesis. Emerg Microbes Infect 6(3):e13. https://doi.org/10.1038/EMI.2016.141
12. Liu ZY, Shi WF, Qin CF (2019) The evolution of Zika virus from Asia to the Americas. Nat Rev Microbiol 17(3):131–139. https://doi.org/10.1038/S41579-018-0134-9
13 Pettersson JH-O et al (2016) How did Zika virus emerge in the Pacific Islands and Latin America? mBio 7(5):e01239-16. https://doi.org/10.1128/MBIO.01239-16
14. Wang L et al (2016) From mosquitos to humans: genetic evolution of Zika virus. Cell Host Microbe 19(5):561–565. https://doi.org/10.1016/J.CHOM.2016.04.006
15. Metsky HC et al (2017) Zika virus evolution and spread in the Americas. Nature 546(7658):411–415. https://doi.org/10.1038/NATURE22402
16. Ye Q et al (2016) Genomic characterization and phylogenetic analysis of Zika virus circulating in the Americas. Infect Genet Evol 43:43–49. https://doi.org/10.1016/J.MEEGID.2016.05.004
17. Althouse BM et al (2016) Potential for Zika virus to establish a sylvatic transmission cycle in the Americas. Plos Negl Trop Dis 10(12):e0005055–e0005055. https://doi.org/10.1371/JOURNAL.PNTD.0005055
18. Vasilakis N, Weaver SC (2017) Flavivirus transmission focusing on Zika. Curr Opin Virol 22:30–35. https://doi.org/10.1016/J.COVIRO.2016.11.007
19. Jenkins GM et al (2002) Rates of molecular evolution in RNA viruses: a quantitative phylogenetic analysis. J Mol Evol 54(2):156–165. https://doi.org/10.1007/S00239-001-0064-3
20. Ciota AT, Kramer LD (2010) Insights into arbovirus evolution and adaptation from experimental studies. Viruses 2(12):2594–2617. https://doi.org/10.3390/V2122594
21. Grubaugh ND, Ebel GD (2016) Dynamics of West Nile virus evolution in mosquito vectors. Curr Opin Virol 21:132–138. https://doi.org/10.1016/J.COVIRO.2016.09.007
22. Moser LA et al (2018) Growth and adaptation of Zika virus in mammalian and mosquito cells. Plos Negl Trop Dis 12(11):e0006880. https://doi.org/10.1371/JOURNAL.PNTD.0006880
23. Deardorff ER et al (2011) West Nile virus experimental evolution in vivo and the trade-off hypothesis. Plos Pathog 7(11):e1002335. https://doi.org/10.1371/JOURNAL.PPAT.1002335
24. van Boheemen S et al (2017) Quasispecies composition and evolution of a typical Zika virus clinical isolate from Suriname. Sci Rep 7(1):2368. https://doi.org/10.1038/S41598-017-02652-W
25. Musso D, Gubler DJ (2016) Zika virus. Clin Microbiol Rev 29(3):487–524. https://doi.org/10.1128/CMR.00072-15
26. Aliota MT et al (2017) Zika in the Americas, year 2: what have we learned? What gaps remain? A report from the Global Virus Network. Antiviral Res 144:223–246. https://doi.org/10.1016/J.ANTIVIRAL.2017.06.001
27 Faye O et al (2014) Molecular evolution of Zika virus during its emergence in the 20(th) century. Plos Negl Trop Dis 8(1):e2636. https://doi.org/10.1371/JOURNAL.PNTD.0002636
28 Faria NR et al (2016) Zika virus in the Americas: early epidemiological and genetic findings. Science (New York, N.Y.) 352(6283):345–349. https://doi.org/10.1371/JOURNAL.PNTD.0002636

29. de Melo Freire CC, et al (2015) Spread of the pandemic Zika virus lineage is associated with NS1 codon usage adaptation in humans [Preprint]. BioRxiv, p 032839. https://doi.org/10.1101/032839
30. Guth S et al (2020) Ecological processes underlying the emergence of novel enzootic cycles: arboviruses in the neotropics as a case study. Plos Negl Trop Dis 14(8):e0008338. https://doi.org/10.1371/JOURNAL.PNTD.0008338
31. Terzian ACB et al (2018) Evidence of natural Zika virus infection in neotropical non-human primates in Brazil. Sci Rep 8(1):16034. https://doi.org/10.1038/S41598-018-34423-6
32. Favoretto SR et al (2019) Zika virus in peridomestic neotropical primates. Northeast Brazil EcoHealth 16(1):61–69. https://doi.org/10.1007/s10393-019-01394-7
33. Favoretto S et al (2016) First detection of Zika virus in neotropical primates in Brazil: a possible new reservoir [Preprint]. BioRxiv, p 049395. https://doi.org/10.1101/049395
34. Vanchiere JA et al (2018) Experimental Zika virus infection of neotropical primates. Am J Trop Med Hyg 98(1):173–177. https://doi.org/10.4269/AJTMH.17-0322
35. Ng WC et al (2017) The 5' and 3' untranslated regions of the flaviviral genome. Viruses 9(6):137. https://doi.org/10.3390/V9060137
36. Queiroz, S.R.d.A., (2011) Estratégias moleculares para utilização do vírus da febre amarela como vetor vacinal. Dissertation, Fundação Oswaldo Cruz - Instituto Aggeu Magalhães. Recife, PE, Brasil.
37. Faye M et al (2020) Biological characteristics and patterns of codon usage evolution for the African genotype Zika virus. Viruses 12(11):1306. https://doi.org/10.3390/V12111306
38. Rosenstierne MW et al (2018) Zika virus IgG in infants with microcephaly, Guinea-Bissau, 2016. Emerg Infect Dis 24(5):948–950. https://doi.org/10.3201/EID2405.180153
39. Bowen JR et al (2017) Zika virus antagonizes type I interferon responses during infection of human dendritic cells. Plos Pathog 13(2):e1006164–e1006164. https://doi.org/10.1371/JOURNAL.PPAT.1006164
40. Weger-Lucarelli J et al (2016) Vector competence of American mosquitoes for three strains of Zika virus. Plos Negl Trop Dis 10(10):e0005101. https://doi.org/10.1371/JOURNAL.PNTD.0005101
41. Lazear HM et al (2016) A mouse model of Zika virus pathogenesis. Cell Host Microbe 19(5):720–730. https://doi.org/10.1016/J.CHOM.2016.03.010
42. Azar SR et al (2017) Differential vector competency of Aedes albopictus populations from the Americas for Zika virus. Am J Trop Med Hyg 97(2):330–339. https://doi.org/10.4269/AJTMH.16-0969
43. Roundy CM et al (2017) Variation in Aedes aegypti mosquito competence for Zika virus transmission. Emerg Infect Dis 23(4):625–632. https://doi.org/10.3201/EID2304.161484
44. Simonin Y et al (2017) Differential virulence between Asian and African lineages of Zika virus. Plos Negl Trop Dis 11(9):e0005821–e0005821. https://doi.org/10.1371/JOURNAL.PNTD.0005821
45 Haddow AD et al (2012) Genetic characterization of Zika virus strains: geographic expansion of the Asian lineage. Plos Negl Trop Dis 6(2):e1477. https://doi.org/10.1371/JOURNAL.PNTD.0001477
46. Laiton-Donato K et al (2019) Complete genome sequence of a Colombian Zika virus strain obtained from BALB/c mouse brain after intraperitoneal inoculation. Microbiol Resour Announc 8(46):e01719-e1818. https://doi.org/10.1128/MRA.01719-18
47. Shrivastava S et al (2018) Whole genome sequencing, variant analysis, phylogenetics, and deep sequencing of Zika virus strains. Sci Rep 8(1):15843. https://doi.org/10.1038/S41598-018-34147-7
48. Strottmann DM et al (2019) Genetic and biological characterisation of Zika virus isolates from different Brazilian regions. Mem Inst Oswaldo Cruz 114:e190150–e190150. https://doi.org/10.1590/0074-02760190150
49. Alpuche-Lazcano SP et al (2018) Higher cytopathic effects of a Zika virus Brazilian isolate from Bahia compared to a Canadian-imported Thai strain. Viruses 10(2):53. https://doi.org/10.3390/V10020053
50. Ávila-Pérez G et al (2019) A natural polymorphism in Zika virus NS2A protein responsible of virulence in mice. Sci Rep 9(1):19968. https://doi.org/10.1038/s41598-019-56291-4
51. Collins ND et al (2019) Inter- and intra-lineage genetic diversity of wild-type Zika viruses reveals both common and distinctive nucleotide variants and clusters of genomic diversity. Emerg Microbes Infect 8(1):1126–1138. https://doi.org/10.1080/22221751.2019.1645572
52. Wang B et al (2018) Structure and function of Zika virus NS5 protein: perspectives for drug design. Cell Mol Life Sci 75(10):1723–1736. https://doi.org/10.1007/s00018-018-2751-x
53. Upadhyay AK et al (2017) Crystal structure of full-length Zika virus NS5 protein reveals a conformation similar to Japanese encephalitis virus NS5. Acta Crystallogr Section F, Struct Biol Commun 73(Pt 3):116–122. https://doi.org/10.1107/S2053230X17001601
54. Zhao B et al (2017) Structure and function of the Zika virus full-length NS5 protein. Nat Commun 8(1):14762. https://doi.org/10.1038/ncomms14762
55 Longdon B et al (2014) The evolution and genetics of virus host shifts. Plos Pathogens 10(11):e1004395. https://doi.org/10.1371/JOURNAL.PPAT.1004395
56. Bahir I et al (2009) Viral adaptation to host: a proteome-based analysis of codon usage and amino acid preferences. Mol Syst Biol 5:311. https://doi.org/10.1038/MSB.2009.71
57 Wang H et al (2016) Analysis of synonymous codon usage bias of Zika virus and its adaption to the hosts. Plos One 11(11):e0166260. https://doi.org/10.1371/JOURNAL.PONE.0166260
58. Hall TA (1999) BioEdit : a user-friendly biological sequence alignment editor and analysis program for Windows 95/98/NT. Nucleic Acids Symp Ser 41:95–98
59. TM Calculator. (s.d.). Protein Melting Temperature Calculation. https://tmcalculator.neb.com/#!/main
60. Sanger F, Nicklen S, Coulson AR (1977) DNA sequencing with chain-terminating inhibitors. Proc Natl Acad Sci U S A 74(12):5463–5467. https://doi.org/10.1073/PNAS.74.12.5463